



Iranian Research Organization
for Science and Technology
(IROST)

Advances
Environmental
Technology



Journal home page: <https://aet.irost.ir>

A numerical study for gas–solid reactions in a microwave-based system: Kinetic and environmental aspects

Kianoosh Shojae, Behnam Khoshandam*

Faculty of Chemical, Petroleum, and Gas Engineering, Semnan University, Semnan, Iran.

ARTICLE INFO

Document Type:
Research Paper

Article history:
Received 29 October 2025
Received in revised form
12 May 2026
Accepted 13 May 2026

Keywords:
Microwave-based reaction
Gas-solid reaction modelling
Carbon emissions
Exact calculation

ABSTRACT

Due to increasing environmental concerns and requirements, the adoption of modern heating methods is strongly recommended. The microwave-based system has attracted considerable attention due to its efficiency, low carbon footprint, low energy consumption, and short process timing. Our studies on microwave heating for synthesizing cobalt and various alloys showed a significant need for novel predictors to model microwave heating processes. This paper is novel in its evaluation of the performance of outstanding numerical methods for solving microwave-based reactions in both kinetic and environmental aspects. As a case study, the experimental results related to the reaction of cobalt metal oxide with syngas under microwave heating were compared to the orthogonal collocation outcomes, and outstanding results were reported with a mean error lower than 5%. The emissions from a microwave and an electrical furnace, based on kinetic values, were also compared. To evaluate numerical methods for different types of reactions in the mentioned microwave heating process, the governing equations from the modeling of gas-solid catalyzed reactions with different reaction orders were solved using the perturbation and orthogonal collocation methods. The environmental analysis demonstrated that the microwave process offered notable environmental and operational advantages over the furnace process, including significantly faster CO removal, more controllable CO₂ emissions, higher energy efficiency, and a reduced overall carbon footprint by possibly reducing energy consumption

1. Introduction

Microwave-assisted reactions in the case of high-temperature gas-solid reaction, particularly, offer significant advantages, including reduced reaction times, improved yields, and enhanced product

purity [1]. This technique has been shown to have many advantages, including rapid and uniform heating, making chemical processes more energy-efficient and environmentally friendly [2]. The high-temperature chemical processes in microwave-based systems are very complex since

*Corresponding author Tel.: +98 9125466376

E-mail: Bkhoshandam@semnan.ac.ir

DOI: 10.22104/aet.2026.7820.2238

COPYRIGHTS: ©2026 Advances in Environmental Technology (AET). This article is an open access article distributed under the terms and conditions of the Creative Commons Attribution 4.0 International (CC BY 4.0) (<https://creativecommons.org/licenses/by/4.0/>)

the reaction degree in these systems is complex [3]. Hence, the use of new numerical and exact methods can be helpful to solve the equations obtained from the modeling of these systems.

Recently, different applications of microwave-based systems have been highlighted for many applications in terms of environmental aspects. Khan, Panda [4] synthesized high-entropy alloy (HEA) nanoparticles using an ultra-efficient pulse microwave method at $\sim 100^\circ\text{C}$ without external heat treatment, achieving uniform 4–10 nm dispersion on graphene oxide sheets. Veronesi, Rosa [5] suggested a microwave-assisted powder metallurgy method for synthesizing high-entropy alloys, demonstrating a significant reduction in energy consumption compared to conventional melting or prolonged solid-state processes. Moreover, the performance of microwave-based systems has been evaluated and examined in many applications [6, 7]. However, it appears that the environmental impact assessment of this system requires further investigation.

Many mathematical and numerical methods have been suggested to solve the governing nonlinear differential equations that can be obtained from the gas-solid reaction. Among different techniques to solve nonlinear differential equations, approximate methods are very desirable [8-10]. The perturbation method is among the preferred approximate methods that have been used in evaluating nonlinear models. Various equations, such as algebraic and integrals, can be solved approximately using the perturbation method. However, a major limitation of this technique is that it generates a small parameter (ε) in the equation, which causes the results to be valid only for weak nonlinear forms of equations. To remove this limitation, the orthogonal collocation or modified Lindstedt-Poincaré methods can be useful [11, 12]. In [13], a new homotopy perturbation method was proposed that did not require a small parameter in the equation; the results showed a good agreement with exact data. The orthogonal collocation method can be employed for solving various chemical engineering problems, such as the Stefan–Maxwell diffusion [14], flow modeling for Newtonian fluids [15], and reaction-diffusion problems [16, 17]. This method is also proper for solving effectiveness factor problems. The use of

two-term orthogonal collocation method for isothermal pellets demonstrated appropriate results [18]. Skoneczny et al. [19] modeled the two types of continuous bioreactors, showing that the mathematical model made using the orthogonal collocation method provided a good agreement compared to the exact data. Nategh et. al. [20] used the orthogonal collocation method to solve the governing equations in dual porosity reservoirs and provided an appropriate result. In [21], scholars solved six chemical engineering problems by utilizing the Chebyshev orthogonal collocation method. They obtained a good agreement between the predicted and exact data, showing that this method can be appropriately used for the elucidation of problems. In [22], scholars evaluated the effects of non-linear convection along with an induced magnetic field in the flow of viscous fluid onto a porous plate. They provided a subject non-linear problem demonstrated in the form of a non-dimensionalized relation. In addition, they solved this relation by means of the perturbation method. By using the perturbation method, it was determined that the magnetic field could highly improve the thermal field, but it could also decrease the velocity field; this method provided a reasonable solution [22]. In [23], scholars showed that the homotopy perturbation method (HPM) was a proper option to solve the singular Duffing-like oscillator. In [24], scholars provided an approximate-analytical solution for PDE problems utilizing adaptable fractional derivatives. However, in the literature, numerical methods, such as perturbation and orthogonal collocation, have not been appropriately evaluated for gas-solid reactions in different systems, especially microwave systems.

After reviewing studies related to the use of the microwave heating process to synthesize cobalt and different alloys [3, 25], it was found that there is a considerable need for new predictors to deal with the equations from microwave heating modeling processes. Hence, this novel work has concentrated on the use of different numerical methods to calculate and estimate the problems related to the microwave heating process. In addition, the prediction of environmental effects along with the kinetic behavior of microwave ovens and common furnaces was evaluated. The

performance of advanced numerical methods for solving microwave-based reaction problems was evaluated with a focus on kinetic and environmental aspects. As a case study, the experimental results for the reaction of cobalt metal oxide with syngas under microwave heating were compared with orthogonal collocation predictions, yielding outstanding agreement with a mean error below 5%. Subsequently, the emissions from the microwave and an electric furnace were compared based on kinetic values. Furthermore, to assess the numerical methods for various types of reactions in microwave heating, the governing equations for gas–solid catalyzed reactions with different reaction orders were solved using perturbation and orthogonal collocation methods.

2. Materials and methods

Figure 1 shows the considered model related to the reaction of metal oxide with gaseous products in a microwave oven. In this model, a metal oxide grain is placed in a microwave oven in which a gaseous flow of hydrogen is diffused into the metal oxide grain. The temperature rising trend and detailed information about this system are explained in [25]. Due to the fact that the reaction degree is unknown in the microwave-based system, a (p) degree for the reaction of metal oxide with hydrogen in the microwave system was considered.

2.1. Case study: homogeneous pellet

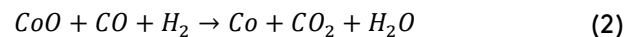
To use the orthogonal collocation method, experimental results for the reaction of cobalt oxide with syngas were considered using the system introduced by Shojae and Khoshandam [3]

that predicted the k factor based on the results obtained at 900 °C for 4 min. Note that a preliminary study was conducted to calculate p, and the best value was determined to be 1. Considering the pellet of cobalt oxide as a homogeneous solid, the following equation can be used:

$$-kC^p_A = \frac{dC_A}{dt} \quad (1)$$

The case study considered a homogeneous pellet, which cannot be generalized to all cases; therefore, it was decided to investigate other geometries and conditions as well.

The main reaction for the reduction of Co from CoO is considered as follows:



To calculate the CO₂ and CO, the following assumptions were considered:

- First-order reaction with respect to CoO concentration.
- Ideal reactor (for both the microwave and furnace), perfectly mixed system, uniform concentrations.

2.1.1. Analytical solution

Eqs. 3, 4, and 5 show the time-dependent concentrations of chemical species in reaction 2. Eq. 3 demonstrates that the concentration of CoO decreases exponentially over time, indicating a first-order reaction with rate constant k. In Eq. 4, the remaining concentration of CO is expressed as the initial concentration minus the consumed amount of CoO, again reflecting first-order kinetics.

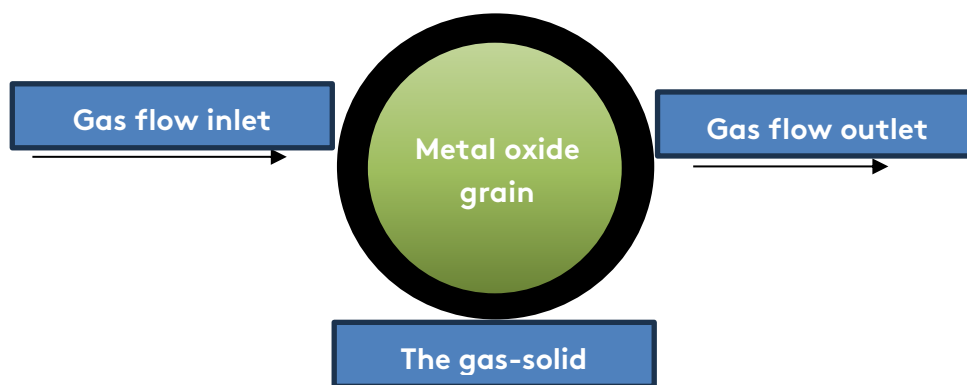


Fig. 1. The model related to the reaction of metal oxide with gaseous product in a microwave oven [26].

Eq. 5 also illustrates that the formation of CO₂ follows the same exponential pattern as the consumption of CoO, implying a direct stoichiometric relationship between CoO consumption.

$$[CoO](t) = C_{Co_0} \times e^{-kt} \quad (3)$$

$$[CoO](t) = C_{Co_0} - C_{Co_0} \times (1 - e^{-kt}) \quad (4)$$

$$[CO_2](t) = C_{Co_0} \times e^{-kt} \quad (5)$$

2.1.2. Orthogonal collocation approach

The governing equations of the model were transformed into a system of ODEs using the orthogonal collocation method. In this study, the spatial domain was discretized using orthogonal collocation on finite elements. The dependent variable $y(z, t)$ was approximated as a linear combination of basis polynomials defined at predefined collocation points. By enforcing the governing equations at these collocation points, the original spatial derivatives were replaced with algebraic expressions, yielding a set of time-dependent ODEs of the general form.

$$dy/dt = f(y, t) \quad (6)$$

The kinetic model is governed by a first-order ordinary differential equation:

$$\frac{dC}{dt} = -kC \quad (7)$$

Using orthogonal collocation, the concentration $C(t)$ is approximated by a polynomial expansion over N collocation points:

$$C(t) \approx \sum_{j=1}^N a_j \phi_j(t) \quad (8)$$

where $\phi_j(t)$ are Lagrange interpolation polynomials defined at the collocation points t_i . Substitution into the governing equation and enforcing it at each collocation point gives:

$$\sum_{j=1}^N D_{ij} C_j = -kC_i, i = 1, \dots, N \quad (9)$$

where D_{ij} is the orthogonal collocation differentiation matrix.

2.1.3. Segmenting the domain

Based on segmenting the domain over small-time segments, the time domain was first divided into n_{seg} equal subintervals with a width of:

$$\Delta t = (t_{final} - t_0)/n_{seg} \quad (10)$$

Then, $y(t)$ was separately approximated in each subinterval by considering τ so that t was mapped to a local variable as $\tau \in [-1, 1]$.

- Endpoints: $\tau = -1$ and $\tau = +1$
- Interior points: roots of the derivative of the legend re polynomial $P_N(\tau)$

2.1.4. Polynomial approximation

To approximate $y(\tau)$ inside each subinterval using an N order of the Lagrange polynomial, the following can be obtained:

$$y(\tau) \approx \sum_{j=1}^{N+1} y_j * L_j(\tau) \quad (11)$$

where $L_j(\tau)$ are Lagrange basis functions:

$$L_j(\tau) = \prod_{m=1, m \neq j}^{N+1} \frac{(\tau - \tau_m)}{(\tau_j - \tau_m)} \quad (12)$$

The coefficients τ_j are simply the values at the collocation points.

2.2. Heterogeneous pellet

For modeling the gas-solid catalyzed reaction in a slab, cylinder, and sphere catalyst, a reactant in the fluid phase should first diffuse through the static boundary layer around the catalyst particle [10]. The Stefan- Maxwell equation introduces this mode of transport as follows:

$$\nabla X_i = \sum_{\substack{j=1 \\ j \neq i}}^n \frac{1}{CD_{ij}} (X_i - N_j - X_j N_i) \quad (13)$$

where C is the total concentration, X_i is the mole fraction of component i , and N_i and N_j are the fluxes of i and j components, respectively. It is known that by considering the equimolar counter-diffusion for two components of A and B ($N_A = -N_B$), Eq.1 reduces to:

$$N_A = -D_{AB} \nabla C_A \quad (14)$$

The reaction in the solid catalyst is considered as follows:

$$C \xrightarrow{k} \text{Prouducts } r_A = kC_A^P \quad (15)$$

Note that the reaction rate was presented in the results and discussion section. The mass balance equation for the catalyst is as follows:

$$N_{A_z} \cdot S - N_{A_{z+\Delta z}} \cdot S - r_A \cdot dV = 0 \quad (16)$$

where S is the catalyst surface and p is considered to be the order of the reaction. Figure 2 shows a schematic of the differential control volume used for the axial mass balance of species A over the catalyst surface.

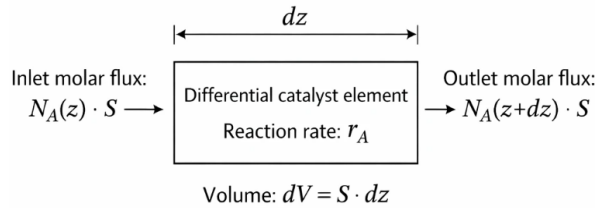


Fig. 2. A schematic of the differential control volume used for the axial mass balance of species A over the catalyst surface.

The boundary conditions have been considered as follows:

$$r = 0, \frac{dc_A}{dr} = 0, r = w, C_A = 1 \quad (17)$$

where C and C_0 are the reactant and bulk concentrations, respectively, and w is the half-thickness of the catalyst.

Defining the non-dimensional parameters ($y = \frac{c}{c_0}$, $x = \frac{r}{w}$):

$$\frac{d^2y}{dx^2} - \varphi_1^2 y^p = 0 \quad (18)$$

$$\frac{d^2y}{dx^2} + \frac{1}{x} \frac{dy}{dx} - \varphi_2^2 y^p = 0 \quad (19)$$

$$\frac{d^2y}{dx^2} + \frac{2}{x} \frac{dy}{dx} - \varphi_3^2 y^p = 0 \quad (20)$$

where φ is $\frac{kc_0^p w^2}{D_{AB} c_0}$.

2.2.1. Slab, cylindrical, and spherical catalysts

In this section, the perturbation and the orthogonal collocation methods are evaluated for slab, cylinder, and sphere catalysts. Boundary conditions (in dimensional form) are considered as follows:

$$\text{B.C.1 } x = 0, \frac{dy}{dx} = 0 \quad (21)$$

$$\text{B.C.2 } x = 1, y = 1 \quad (22)$$

In this section, the modeling of a first-order reaction in a flat catalyst is examined. In the first step, the governing differential equation for the system is derived, and by changing the variable

from x to $u = x^2$, a simpler form of the equation is taken into consideration. Then, using Lagrange polynomials, the value of the function at different points is approximated. For summarization, these procedures are not presented here. The boundary conditions, such as the function value at the edges, are taken into account; by using Jacobi polynomials for the low-degree cases of $g=2, N=1, g=2$, and $g=N=2$, simplified equations are specifically derived to allow for the approximate calculation of the function value at specific points.

Substituting these parameters in Eq. 18 yields:

$$u_1 = x_1^2 = 0 \cdot 5853 \text{ and } u_2 = x_1^2 = 0 \cdot 0813$$

Eq. 23 shows the trial function considered for the perturbation method [9].

$$y = y_0 + \varepsilon y_1 + \dots$$

$$\left(\frac{d^2 y_0^o}{dx^2} + \varepsilon \frac{d^2 y_1^o}{dx^2} + \dots \right) - \frac{1}{\varepsilon^2} (y_0^o + \varepsilon y_1^o + \dots)^p = 0 \quad (23)$$

where ε is a small number. It should be noted that the φ and y^p parameters can be rewritten with the Taylor series.

The Eq. 23 is a singular problem. Considering the boundary layer near $x=1$, for the outer solution taking into account B.C.1 and B.C.2 yields:

$$O(\varepsilon^0): y_0^o = 0$$

$$O(\varepsilon^1): y_1^o = 0$$

$$O(\varepsilon^2): y_0^o = 0$$

Because the boundary layer is near $x=1$, Eq. 23 should be rewritten considering the following variable change:

$$x^* = \frac{1-x}{\varepsilon^n} \quad (24)$$

Boundary conditions change to [9]:

$$\text{B.C.3: } x^* = 0 \quad y = 1 \quad (25)$$

$$\text{B.C.3: } x^* = \infty \quad \frac{dy}{dx^*} = 0$$

For $n=1$, Eq. 23 reduces to:

$$\left(\frac{d^2 y_0^i}{dx^{*2}} + \varepsilon \frac{d^2 y_1^i}{dx^{*2}} \right) - (y_0^i + \varepsilon y_1^i)^p = 0 \quad (26)$$

2.2.2. The perturbation method

For $p=1$, the problem becomes the simplest form and can be solved with B.C.3 and B.C.4 as:

$$O(\varepsilon^0): y_0^i = \exp(-x^*) \tag{27}$$

Using the common perturbation method yields:

$$y = y_0^i = \exp(-x^*) \tag{28}$$

Using the zero-order perturbation method, a general solution is obtained as follows:

$$O(\varepsilon^0): y_0^{i(0.5-0.5p)} = -(0.5 - 0.5p) \cdot \left(\frac{1}{p+1}\right)^{0.5} \cdot x^* + 1 \tag{29}$$

$$y = y_0^i$$

When the chemical reaction is not the controlling step, problem (Eq. 23) can be solved by the regular perturbation method as follows:

$$O(\varepsilon^0): y_0(x) = 1$$

$$O(\varepsilon^1): y_1(x) = 10 O(\varepsilon^2): y_2(x) = \frac{1}{4}x^2 + \frac{3}{4} \tag{30}$$

$$O(\varepsilon^3): y_3(x) = \frac{1}{4}px^2 + 1 - p \frac{1}{4}$$

In the same way, using the regular perturbation method for sphere geometry gives:

$$O(\varepsilon^0): y_0(x) = 1 \tag{31}$$

$$O(\varepsilon^1): y_1(x) = 1$$

$$O(\varepsilon^2): y_2(x) = \frac{1}{6}x^2 + \frac{5}{6}$$

$$O(\varepsilon^3): y_3(x) = \frac{1}{6}px^2 + 1 - p * \frac{1}{6}$$

3. Results and discussion

3.1. Case study

The kinetics of reaction

As mentioned previously, the best reaction order was found to be 1 (p=1). Figure 3 shows the comparison of the results related to the mentioned reaction in the form of orthogonal collocation. The error for the calculation of cobalt oxide (CoO) reduction amount by the orthogonal collocation method is lower than 5 %, demonstrating its outstanding result for the calculation in the microwave-based system.

For calculating the k factor for the microwave reaction, a comparison between the microwave-based reaction and an in-furnace reaction of CoO at a temperature of about 700 °C [27] was performed, and the results are presented in Table 1.

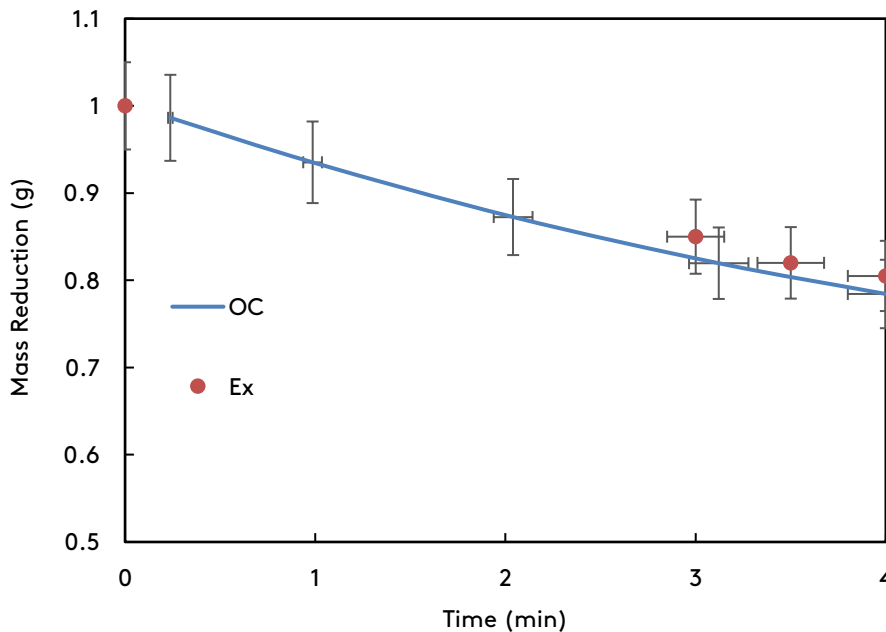


Fig. 3. The comparison of orthogonal collocation (OC) results compared to the experimental ones ($k \cong 0.57 \frac{1}{min}$).

Table 1. The k value predicted by the orthogonal collocation method and experimental results from [27].

Temperature	Predicted k for furnace (1/min)	Predicted k for microwave (1/min)
700 °C	$\cong 0.0069$	0.21

As can be seen in Table 1, the k for the microwave system is higher than that of the conventional heating system. This difference can be attributed to the distinct heating mechanisms of microwave heating due to its rapid and volumetric energy absorption; non-uniform temperature distribution and localized overheating caused the overall reaction efficiency to be reduced. In contrast, conventional heating relies on slower, surface-to-core heat transfer, resulting in more uniform temperature profiles that favor consistent reaction rates [3, 25]. In addition, the microwave system may induce different reaction pathways or intermediate formations, affecting the observed rate constants.

3.1.1. The environmental aspects

Figure 4 demonstrates a comparison between experimental data [28] related to the CO generation of experimental and predicted data. As can be seen, there is an acceptable agreement between the experimental and simulated data related to the gasification of 1 mol glycerol to CO and CO₂. Figures 5 and 6 show a comparison of the CO₂ and CO emissions from the microwave and furnace processes, respectively. As seen, the microwave process significantly reduced the residence time of CO in the system, consumed and converted to CO₂ much earlier compared to furnace operation. The concentration of CO as a toxic and polluting gas decreased to about zero much faster, lowering both the toxic risk to workers and its release into the atmosphere. In microwave

systems, the shorter reaction time and smaller overall process volume allowed easier capture or neutralization of the CO₂ produced.

In contrast, the furnace generated CO₂ over a longer period and at a lower rate, making emissions more continuous and harder to control. Furthermore, the introduced microwave heating process (Figure 1) also delivers higher energy efficiency by generating heat directly within the material that caused heat loss compared to conventional furnaces. As a result, the same level of conversion can be achieved with less energy consumption, thereby decreasing fossil fuel use and indirectly lowering emissions. The high processing kinetics of the microwave process enabled fine control of reaction stoppage to minimize excess CO₂ production. Figure 7 shows a comparison related to the time-integrated emissions of CO and CO₂ for the conventional furnace and microwave-assisted reduction processes. The results indicate that CO emissions are substantially higher in the furnace, reaching nearly 4 mol·min, compared to about 3 mol·min for the microwave process, representing a reduction of approximately 20–25%. However, in cases of CO₂ emissions, the microwave process produces slightly more value than the furnace, but still at levels close to zero. These findings suggest that microwave heating offers a significant environmental advantage by reducing toxic CO emissions, while the small increase in CO₂ is negligible compared to the overall improvement in gaseous emission profiles.

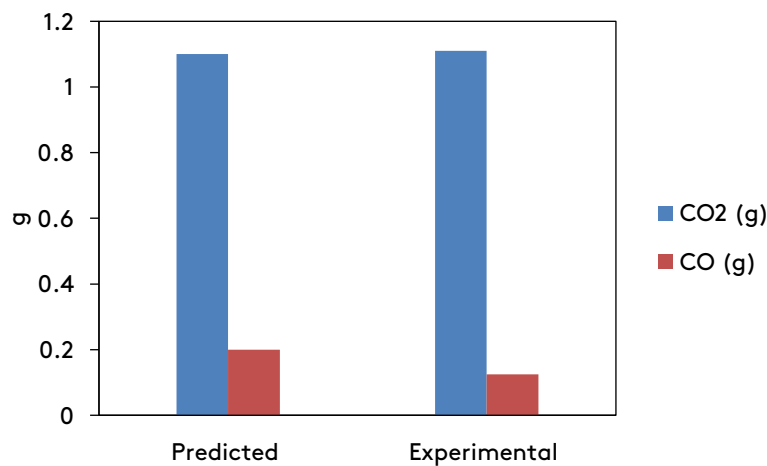


Fig. 4. The experimental data [28] versus the predicted ones related to the gasification of 1 mol Glycerol.

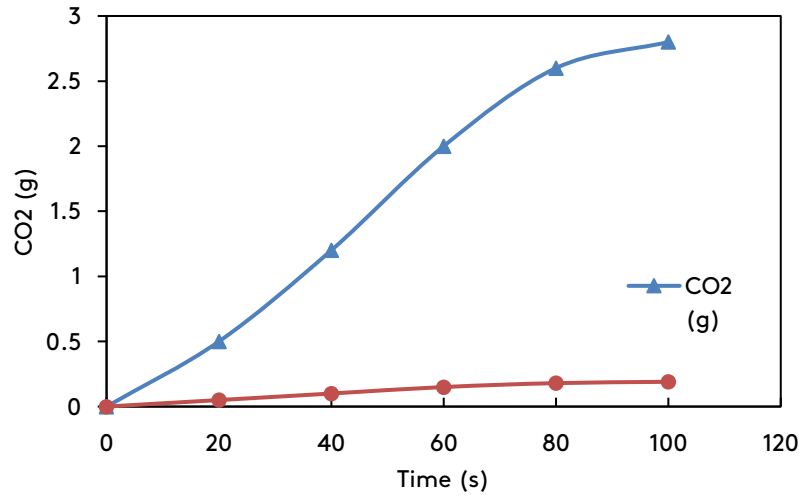


Fig. 5. CO₂ concentration over time for furnace and microwave processes.

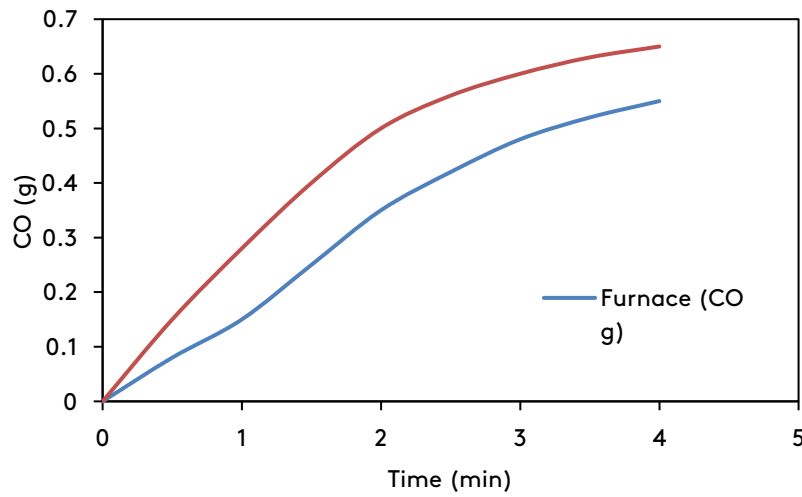


Fig. 6. CO concentration over time for furnace and microwave processes. The use of a microwave system led to an increase in CO production over a common furnace.

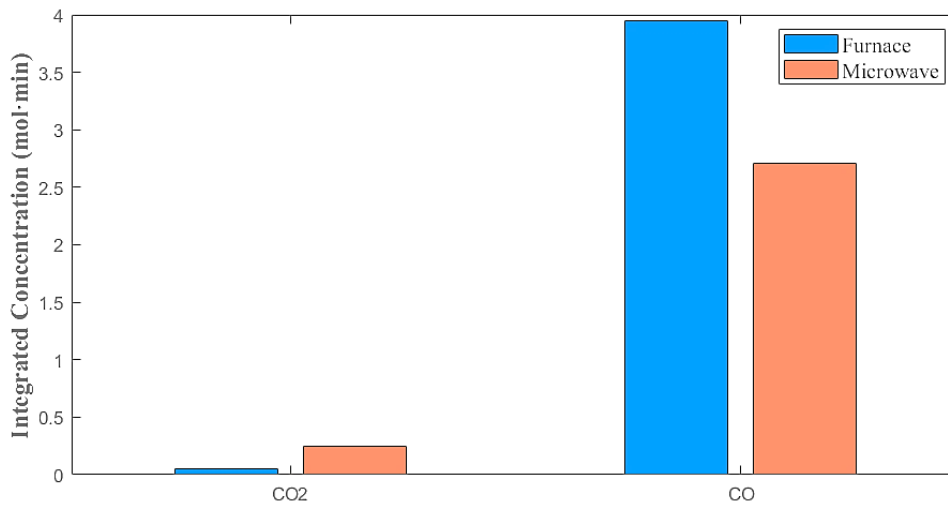


Fig. 7. Time-integrated CO and CO₂ emissions for furnace and microwave processes.

3.2. Different geometries and conditions

The use of $N=5$ for the orthogonal collocation method, considering B.C.2 (for u_5 and y_5), was considered to solve the non-linear five unknowns and five equations created by setting the reaction order to 1.5 or 2.5. The calculations were performed and are presented in Figure 8. As illustrated, by taking advantage of the orthogonal collocation method ($N=5$), the exact solution can be approximately obtained, and increasing the reaction order does not affect the method accuracy. It is found that for solving the presented slab geometry equation by setting N to 5, the equation can be exactly solved for any order of reaction, and increasing the number of collocation points, N , is not needed. Further investigations

show that by changing the φ_1^2 parameter, the same accuracy is achieved for the orthogonal collocation method.

Although solving the problems calculated by the orthogonal collocation method has given almost the exact solution, using the perturbation method can be very effective due to the reduction of computational cost. For this reason, the governing equation from the modeling of the slab catalyst has also solved with the perturbation method. Figure 9 shows the results obtained by using the zero-order perturbation method. As seen, for $p=1$ and $p=2.5$, the calculated and the exact solutions are in good agreement with each other; without calculating y_0^i , the reaction orders of 1.5 and 2.5 mean errors were created by around 3%.

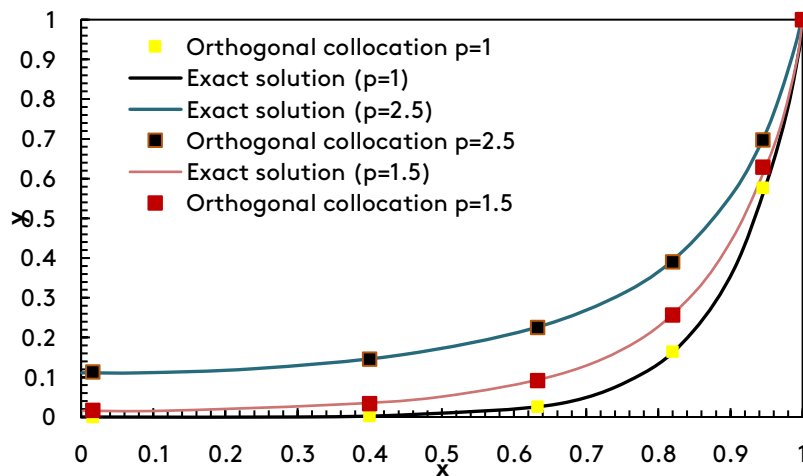


Fig. 8. Comparison of calculated solution (by the orthogonal collocation method) and exact data for the slab catalyst and the different reaction orders of 1, 1.5, and 2.5.

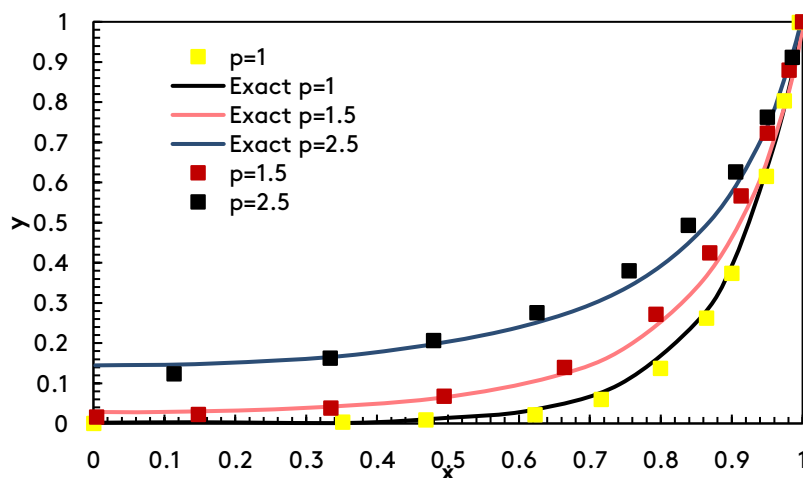


Fig. 9. Comparison of calculated solution (by the perturbation method) and exact data for the slab geometry and the different reaction orders of 1, 1.5, and 2.5.

If more accuracy is required, further terms (y_1^i, y_2^i, y_3^i , etc.) should be additionally calculated in the same way for any problems, such as the considered equation. Table 2 denotes a comparison of calculated and exact solutions.

Table 2. Comparison of calculated and exact solutions when the chemical reaction is not the controlling step for the order reaction of 1, 1.5, and 2.5.

Order (p)	Average Error (%)
1.0	0.32
1.5	0.25
2.5	0.32

As seen, the computational error is under 0.5% for the different reaction orders of 1, 1.5, and 2.5 and is usable for any order of reaction when the φ

parameter is a small number. In the same way, based on the provided results in Figure 10, the orthogonal collocation method with a polynomial degree of 5 was employed for the cylinder geometry. Figure 10 illustrates the calculated and the exact results. As seen, the same accuracy as the data is yielded, and the orthogonal collocation gives almost the exact solution. Figure 11 shows a comparison of the exact and calculated data for various orders of reactions. As seen, for the reaction orders of 1 and 1.5, the mean errors caused by calculating the problem with the perturbation method compared to the exact data (for the trial function of $y = y_0 + \varepsilon y_1$) are zero. Considering the perturbation method and trial function of $y = y_0$ for a 2.5 reaction order, the mean error is high.

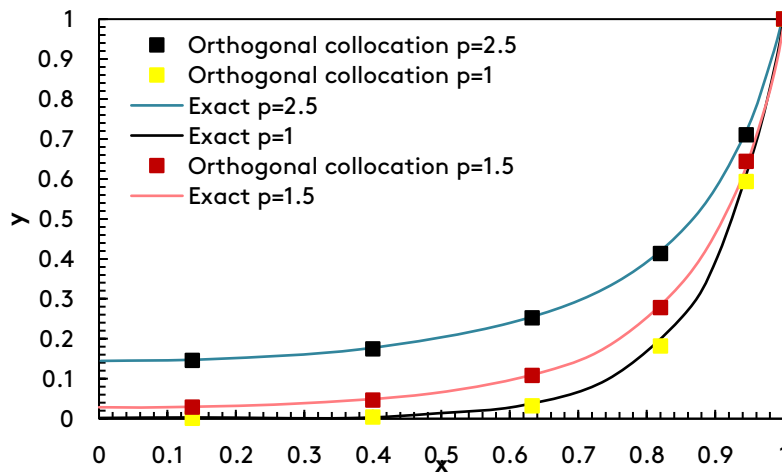


Fig. 10. Comparison of calculated data (by the orthogonal collocation method) and exact solutions for the cylinder geometry and the reaction orders of 1, 1.5, and 2.5.

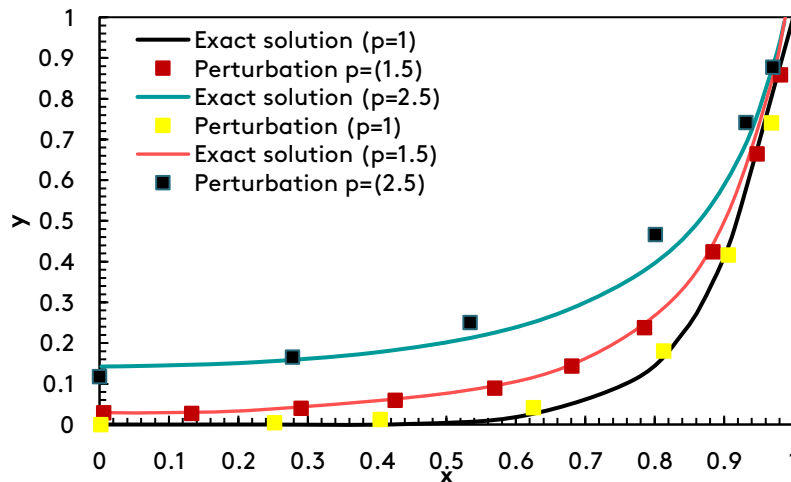


Fig. 11. Comparison of calculated data (by the perturbation method) and exact solutions for the cylinder geometry and the reaction orders of 1, 1.5, and 2.5.

This trial function was used for a reaction order of 2.5 because including the y_1 term creates a complex equation that can only be solved numerically.

Table 3 shows a comparison of calculated and exact solutions for various reaction orders when φ is a small parameter. As illustrated, the regular perturbation method is proper when φ is a small number, and for the different reaction orders of 1, 1.5, and 2.5, errors are by 1%.

Table 3. Comparison of calculated and exact solutions for the order reaction of 1, 1.5, 2.5. When the chemical reaction is not the controlling step.

Order (p)	Average Error (%)
1.0	1.01
1.5	1.01
2.5	1.01

In this section, the emphasis is on an investigation of the accuracy of the orthogonal collocation and the perturbation methods.

Figures 12 and 13 show the obtained data by taking advantage of the orthogonal collocation and the perturbation methods, and the exact solutions were calculated. As determined, using the orthogonal collocation method gives almost the exact results, and the computational errors are about zero percent.

As can be seen in Figure 12, for the reaction order of 1, the calculated results are in good agreement with exact solutions because of considering the trial function of $y = y_0 + \varepsilon y_1$. However, this

agreement is not seen for the reaction order of 1.5 and 2.5 due to the use of the trial function of $y = y_0$. Considering the y_1 parameter in the trial function for these reaction orders yields complex equations and can only be solved by numerical methods.

Table 4 shows a comparison of the predicted and exact data for three reaction orders. As seen in Table 4, created errors are 1% for these reaction orders, and accuracy is not changed by increasing the reaction order.

Table 4. Comparison of calculated and exact solutions when φ is a small number (0.01) for order reactions of 1, 1.5, 2.5 (sphere geometry).

Order (p)	Average Error (%)
1.0	1.01
1.5	1.01
2.5	1.01

When both the chemical reaction and concentration are the controlling step (for a moderate value of φ^2), the regular perturbation method cannot solve the problems because the small value (epsilon in the regular perturbation method) does not exist in the considered problems. Investigations have shown that the orthogonal collocation method is efficient for solving problems with moderate values of φ^2 .

The Figures 14a, 14b, and 14c show the results of the perturbation method for the reaction orders of 1, 1.5, and 2.5, and the value of φ^2 is about 5.

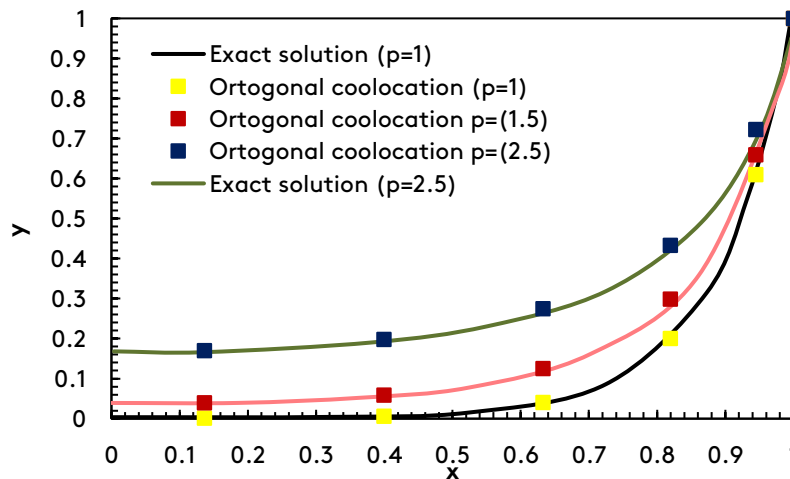


Fig. 12. Comparison of calculated data (by the orthogonal collocation method) and exact solutions for the spherical geometry.

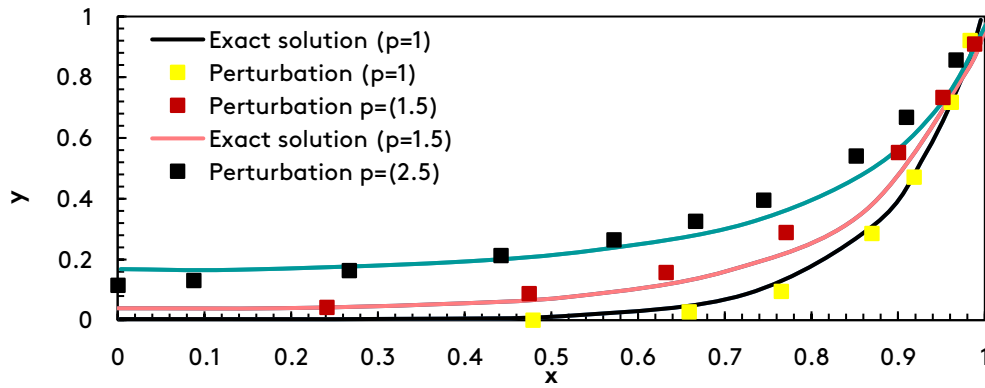


Fig. 13. Comparison of calculated data (by the perturbation method) and exact solutions for the sphere geometry.

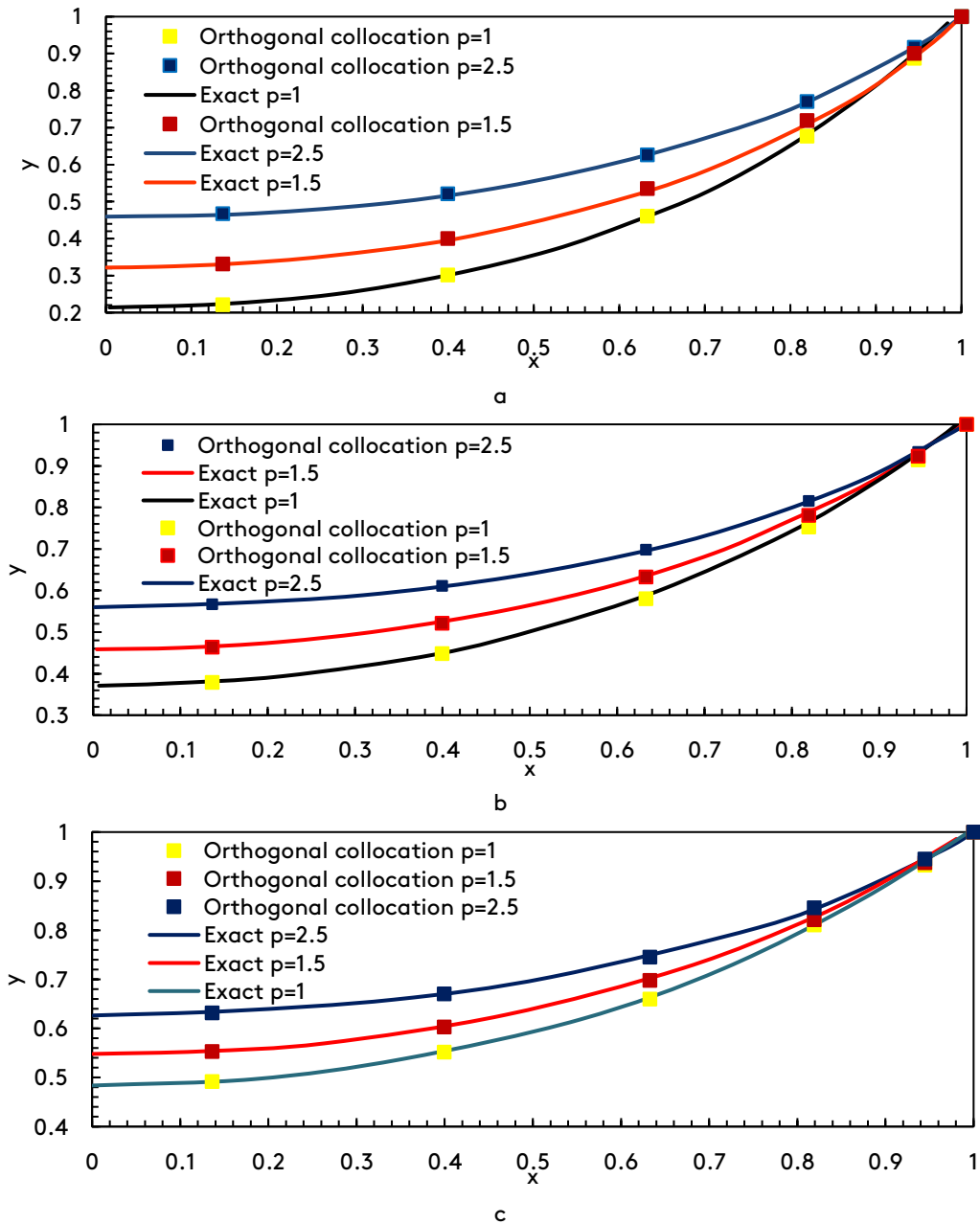


Fig. 14. The perturbation results: (a). Comparison of calculated data and exact solutions for the slab catalyst, (b). the cylindrical catalyst, and (c). the spherical catalyst

4. Conclusion

In recent years, the application of microwave heating in high-temperature gas-solid reactions has offered remarkable potential for improving yield, reducing reaction time, and enhancing product quality. Based on the comparative analysis related to CoO reduction with syngas in a microwave system versus an electric furnace, the higher reaction rate for the microwave process is due to volumetric heating and faster energy transfer. Beyond kinetic advantages, substantial reductions in CO and CO₂ emissions and improved energy efficiency were notable environmental benefits of this approach.

In the case of a modeling perspective, the orthogonal collocation method, even with a limited number of collocation points, showed to have near-exact accuracy across various catalyst geometries (slab, cylindrical, spherical) and a wide range of reaction orders.

As a result of its stability and high precision, this method has been particularly determined to be suitable for problems with moderate to large φ^2 values. In contrast, the regular and modified perturbation methods, while limited by their dependence on a small parameter, provided fast and cost-effective solutions for small- φ conditions and certain nonlinear problems, achieving errors below 1% in many cases. It has also resulted in integrating experimental data with high-accuracy numerical predictions, which not only enabled a detailed kinetic analysis of microwave-assisted reactions but also provided a robust framework for evaluating environmental impacts. The application of this combined approach to design and optimize the industrial microwave systems, particularly for pollutant reduction and energy savings, provides a new approach in developing greener and more sustainable chemical processes.

Nomenclature

Symbols

Symbol	Description	Unit
C	Concentration of reactant	$\text{mol } m^{-3}$
C_A	Concentration of species A (CoO)	$\text{mol } m^{-3}$
C_{A0}	Initial concentration of reactant A	$\text{mol } m^{-3}$
C_{CO}	Carbon monoxide concentration	$\text{mol } m^{-3}$
C_{CO_2}	Carbon dioxide concentration	$\text{mol } m^{-3}$
D_{AB}	Binary diffusion coefficient of species A in B	$m^2 s^{-1}$

k	Reaction rate constant	ss^{-1} or min^{-1}
N_A	Molar flux of species A	$\text{mol } m^{-2} s^{-1}$
N_i, N_j	Molar flux of species i and j	$\text{mol } m^{-2} s^{-1}$
p	Reaction order	-
r_A	Reaction rate of species A	$\text{mol } m^{-3} s^{-1}$
S	Catalyst surface area	m^2
t	Time	s or min
V	Catalyst particle volume	m^3
x	Dimensionless spatial coordinate ($x = r/w$)	-
y	Dimensionless concentration ($y = C/C_0$)	-
w	Half-thickness or radius of catalyst particle	m
ϕ	Thiele modulus	-
ε	Small perturbation parameter	-
τ	Local dimensionless time variable used in collocation	-
z	Axial coordinate	m

Subscripts and indices

Symbol	Description
0	Initial value
A	Reactant species
i, j	Chemical species index

Abbreviations

Abbreviation	Description
OC	Orthogonal Collocation
MW	Microwave
EF	Electric Furnace
ODE	Ordinary Differential Equation

Acknowledgement

The authors would like to acknowledge Semnan University for its support and funding under contract number 23598.

Author's contribution

The manuscript was prepared and written collaboratively by the author and the supervisor. Both contributed to the development of the content and approved the final version. All authors have read and approved the final version of the manuscript.

Conflict of interest

No potential conflict of interest was reported by the authors.

Data availability

Data are not publicly available due to Semnan University restrictions, but can be requested from the corresponding author.

Funding

Support and funding were from Semnan University under contract number 23598.

References

- [1] Li, Z., et al. (2025). Advanced mechanisms and applications of microwave-assisted synthesis of carbon-based materials: A brief review. *Nanoscale Advances*.
<https://doi.org/10.1039/d4na00701h>
- [2] Palma, V., et al. (2020). Microwaves and heterogeneous catalysis: A review on selected catalytic processes. *Catalysts*, 10(2), 246.
- [3] Shojae, K., & Khoshandam, B. (2021). A novel two-step fixed bed reactor for the reduction of cobalt oxide under microwave heating. *Materials Science and Engineering: B*, 267, 115085.
<https://doi.org/10.1016/j.mseb.2021.115085>
- [4] Khan, J. B., et al. (2024). Microwave synthesis of high-entropy alloy catalysts on graphene oxide sheets for oxygen reduction and evolution reactions. *International Journal of Hydrogen Energy*, 53, 999-1008.
<https://doi.org/10.1016/j.ijhydene.2023.12.024>
- [5] Veronesi, P., et al. (2015). Microwave-assisted preparation of high entropy alloys. *Technologies*, 3, 182-197.
<https://www.mdpi.com/2227-7080/3/4/182>
- [6] Loharkar, P. K., Ingle, A., & Jhavar, S. (2019). Parametric review of microwave-based materials processing and its applications. *Journal of Materials Research and Technology*, 8(3), 3306-3326.
<https://doi.org/10.1016/j.jmrt.2019.04.004>
- [7] Li, J., et al. (2021). Review of microwave-based treatments of biomass gasification tar. *Renewable and Sustainable Energy Reviews*, 150, 111510.
<https://doi.org/10.1016/j.rser.2021.111510>
- [8] Jafari, H., & Tajadodi, H. (2016). Electro-spun organic nanofibers elaboration process investigations using BPs operational matrices. *Iranian Journal of Mathematical Chemistry*, 7(1), 19-27.
<https://doi.org/10.22052/ijmc.2016.11866>
- [9] Chen, L., et al. (2017). A two-level stochastic collocation method for semilinear elliptic equations with random coefficients. *Journal of Computational and Applied Mathematics*, 315, 195-207.
<https://doi.org/10.1016/j.cam.2016.10.030>
- [10] Jayakumar, J., & Ramanujam, N. (1994). A numerical method for singular perturbation problems arising in chemical reactor theory. *Computers & Mathematics with Applications*, 27(5), 83-99.
[https://doi.org/10.1016/0898-1221\(94\)90078-7](https://doi.org/10.1016/0898-1221(94)90078-7)
- [11] Aksoy, Y., & Pakdemirli, M. (2010). New perturbation-iteration solutions for Bratu-type equations. *Computers & Mathematics with Applications*, 59(8), 2802-2808.
<https://doi.org/10.1016/j.camwa.2010.01.050>
- [12] Öztürk, Y., et al. (2013). A collocation method for solving fractional Riccati differential equation. *Journal of Applied Mathematics*, 598083.
<https://doi.org/10.1155/2013/598083>
- [13] He, J.-H. (2000). A coupling method of a homotopy technique and a perturbation technique for non-linear problems. *International Journal of Non-Linear Mechanics*, 35(1), 37-43.
[https://doi.org/10.1016/S0020-7462\(98\)00085-7](https://doi.org/10.1016/S0020-7462(98)00085-7)
- [14] Binous, H., & Bellagi, A. (2016). Orthogonal collocation methods using Mathematica® in the graduate chemical engineering curriculum. *Computer Applications in Engineering Education*, 24(1), 101-113.
<https://onlinelibrary.wiley.com/doi/abs/10.1002/cae.21676>
- [15] Binous, H., Shaikh, A. A., & Bellagi, A. (2015). Chebyshev orthogonal collocation technique to solve transport phenomena problems with Matlab® and Mathematica. *Computer Applications in Engineering Education*, 23(3), 422-431.
<https://onlinelibrary.wiley.com/doi/10.1002/cae.21612>
- [16] Housam, B., et al. (2016). Numerical elucidation of three-dimensional problems in the chemical engineering graduate curriculum: Orthogonal collocation. *Computer Applications in Engineering Education*, 24.
<https://onlinelibrary.wiley.com/doi/10.1002/cae.21756>
- [17] Abdelkawy, M., & Alyami, S. (2021). Legendre-Chebyshev spectral collocation method for

- two-dimensional nonlinear reaction-diffusion equation with Riesz space-fractional. *Chaos, Solitons & Fractals*, 151, 111279.
<https://doi.org/10.1016/j.chaos.2021.111279>
- [18] Olatunde, A. O., Olafadehan, O. A., & Usman, M. A. (2020). Computation of effectiveness factor for methanol steam reforming over Cu/ZnO/Al₂O₃ catalyst pellet. *Alexandria Engineering Journal*, 10(1), 35-47.
<https://doi.org/10.1007/s13203-020-00244-w>
- [19] Skoneczny, S., & Cioch, M. (2018). Modeling of continuous-flow bioreactors with a biofilm with the use of orthogonal collocation on finite elements. *Chemical Engineering Science*, 205(7), 929-946.
<https://www.tandfonline.com/doi/full/10.1080/00986445.2018.1423557>
- [20] Nategh, M., Vaferi, B., & Riazi, M. (2018). Orthogonal collocation method for solving the diffusivity equation: Application on dual porosity reservoirs with constant pressure outer boundary. *Journal of Energy Resources Technology*, 141(4).
- [21] Binous, H., Kaddeche, S., & Bellagi, A. (2017). Solution of six chemical engineering problems using the Chebyshev orthogonal collocation technique. *Chemical Engineering Education*, 25(4), 594-607.
<https://onlinelibrary.wiley.com/doi/abs/10.1002/cae.21823>
- [22] Athira, P., et al. (2018). Non-linear convection in chemically reacting fluid with an induced magnetic field across a vertical porous plate in the presence of heat source/sink. In *Defect and Diffusion Forum* (Vol. 389, pp. 55-66). Trans Tech Publ.
- <https://www.scientific.net/DDF.387.428>
- [23] He, J.-H., & El-Dib, Y. O. (2020). Homotopy perturbation method for Fangzhu oscillator. *Journal of Mathematical Chemistry*, 58(10), 2245-2253.
<https://www.scientific.net/DDF.387.428>
 (Note: Duplicate URL; kept as given.)
- [24] Yavuz, M. (2017). Novel solution methods for initial boundary value problems of fractional order with conformable differentiation. *An International Journal of Optimization and Control: Theories & Applications (IJOCTA)*, 8(1), 1-7.
<https://ijocta.org/index.php/files/article/view/540>
- [25] Shojae, K., & Khoshandam, B. (2022). The experimental and modeling study on a new process of iron/cobalt alloy production using indirect reducing agent of glycerol under microwave heating. *Chemical Engineering and Processing - Process Intensification*, 171, 108765.
<https://doi.org/10.1016/j.cep.2021.108765>
- [26] Moghani, M., Beiki, H., & Shojae, K. (2024). Investigating the efficiency of the microwave heating process for the carbothermic synthesis of cobalt/nickel alloys. *Arabian Journal of Chemistry*, 17(2), 105544.
- [27] Bustnes, J. A., Sichen, D., & Seetharaman, S. (1995). Kinetic studies of reduction of CoO and CoWO₄ by hydrogen. *Metallurgical and Materials Transactions B*, 26(3), 547-552.
<https://doi.org/10.1007/BF02653872>
- [28] Javad Nodehi, B. K. (2018). *Pyrolysis of glycerol for syngas production* (Master's thesis? Unclear). Faculty of Chemical, Petroleum and Gas Engineering, Semnan University.

How to cite this paper:



Shojae, K. & Khoshandam, B. (2026). A numerical study for gas-solid reactions in a microwave-based system: kinetic and environmental aspects. *Advances in Environmental Technology*, 12(3), 360-374. DOI: 10.22104/aet.2026.7820.2238